OXFORD

*Human Molecular Genetics*, 2018, Vol. 27, No. 1 30–40

**doi: 10.1093/hmg/ddx381**
Advance Access Publication Date: 12 October 2017
Original Article

ORIGINAL ARTICLE

# Hippocampal phosphorylated tau induced cognitive decline, dendritic spine loss and mitochondrial abnormalities in a mouse model of Alzheimer's disease

Ramesh Kandimalla[1,2], Maria Manczak[1], Xiangling Yin[1], Rui Wang[1,2] and P. Hemachandra Reddy[1,2,3,4,5,6,7,*]

[1]Garrison Institute on Aging, Texas Tech University Health Sciences Center, Lubbock, TX, 79430, USA, [2]Neuroscience & Pharmacology Department, [3]Cell Biology & Biochemistry Department, [4]Neurology Department, [5]Department of Public Health and [6]Speech, Language and Hearing Sciences Departments, Texas Tech University Health Sciences Center, Lubbock, TX 79430, USA and [7]Garrison Institute on Aging, Texas Tech University Health Sciences Center, South West Campus, Lubbock, TX 79413, USA

*To whom correspondence should be addressed at: Mildred and Shirley L. Garrison Chair in Aging, Neuroscience & Pharmacology and Neurology Departments, Texas Tech University Health Sciences Center, 3601 4th Street, MS 9424/4A 124, Lubbock, TX 79430, USA. Tel: 806-743-2393; Fax: 806-743-3636; Email: hemachandra.reddy@ttuhsc.edu

## Abstract

The purpose of our study was to understand the toxic effects of hippocampal phosphorylated tau in tau mice. Using rotarod and Morris water maze (MWM) tests, immunoblotting and immunofluorescence, Golgi-Cox staining and transmission electron microscopy, we assessed cognitive behavior, measured protein levels of mitochondrial dynamics, MAP2, total and phosphorylated tau, and quantified dendritic spines and mitochondrial number and length in 12-month-old tau mice with P301L mutation. Mitochondrial function was assessed by measuring the levels of $H_2O_2$, lipid peroxidation, cytochrome oxidase activity and mitochondrial ATP. MWM and rotarod tests revealed that hippocampal learning and memory and motor learning and coordination were impaired in tau mice relative to wild-type (WT) mice. Increased levels of mitochondrial fission proteins, Drp1 and Fis1 and decreased levels of mitochondrial fusion proteins, Mfn1, Mfn2 and Opa1 were found in 12-month-old tau mice relative to age-matched WT mice, indicating that the presence of abnormal mitochondrial dynamics in tau mice. Decreased levels of dendritic protein, MAP2 and increased levels of total and phosphorylated tau proteins were found in tau mice relative to WT mice. Mitochondrial function was defective. Golgi-Cox staining analysis revealed that dendritic spines are significantly reduced. Transmission electron microscopy revealed significantly increased mitochondrial numbers and reduced mitochondrial length in tau mice. These findings suggest that hippocampal accumulation of phosphorylated tau is responsible for abnormal mitochondrial dynamics and reducing dendritic protein MAP2 and dendritic spines and hippocampal based learning and memory impairments, and mitochondrial structural and functional changes in tau mice. Based on these observations, we propose that reduced hippocampal phosphorylated tau is an important therapeutic strategy for AD and other tauopathies.

**Received:** September 14, 2017. **Revised:** September 28, 2017. **Accepted:** October 9, 2017

## Introduction

Alzheimer's disease (AD) is a progressive, age-dependent neurodegenerative disorder, characterized clinically by the impairment of cognitive functions and changes in behavior and personality (1–5). According to World Alzheimer Report, one in every 3 s, a new case of dementia is being diagnosed in the world. Currently, there are 46.8 million people, including 5.4 million Americans suffer from AD (6). With increasing lifespan in humans, AD is a growing health concern in the society. In addition to the personal and family hardships that AD creates, these numbers translate into extremely high health-care costs. Current estimate health care cost about 818 billion in the world.

AD is associated with phosphorylated tau, neurofibrillary tangles (NFTs) and extracellular amyloid beta (Aβ) plaques in regions of the brain that are responsible for learning and memory (1,3,4,7,8). In addition, AD is also associated with synaptic damage and loss of synapses, abnormal mitochondrial structural and functional alterations and the proliferation of reactive astrocytes and microglia and neuronal loss (1,3–5,9–12).

Increasing evidence suggests that hyperphosphorylation of tau and NFTs are more definitive diagnostic features and tightly linked to cognitive decline in AD patients. However, the structural and functional relevance of hyperphosphorylated tau and NFT to AD is not completely understood. Tau is a major microtubule-associated protein that plays a large role in the outgrowth of neuronal processes and the development of neuronal polarity (7). Tau promotes microtubule assembly, stabilizes microtubules, and affects the dynamics of microtubules in neurons (13–15). Tau is abundantly present in the central nervous system and is predominantly expressed in neuronal axons (16,17).

Normal tau performs several cellular functions, including stabilization of microtubules, promotion of neurite outgrowth, membrane interactions facilitation of enzyme anchoring and facilitation axonal transport of organelles to nerve terminals (7,18). In AD, tau is hyperphosphorylated, becomes pathological, accumulates in neurons, and forms paired helical filaments. As a result, tau loses its capability to bind with microtubules, not able to transport subcellular cellular organelles, such as mitochondria, endoplasmic reticulum, lysosomes and proteins and lipids from soma to nerve terminals—synapses, ultimately leading to synaptic degeneration and cognitive decline in persons with AD. However, the mechanistic links between hippocampal accumulation of hyperphosphorylated tau and cognitive behavioral changes are not completely understood; further, whether links between hippocampal hyperphosphorylated tau-induced dendritic spine loss and cognitive behavioral changes also not clearly understood. In addition, whether hippocampal hyperphosphorylated-tau is critical for mitochondrial dysfunction, particularly ATP levels is not completely understood.

In the current study, we sought to determine (i) hippocampal spatial learning and memory behavioral changes, (ii) total and phosphorylated tau accumulations, (iii) dendritic spine loss, (iv) changes in mitochondrial dynamics proteins, (v) changes in dendritic protein, MAP2, (vi) mitochondrial structural and functional changes in the hippocampal region of 12-month-old tau transgenic mice—P301L strain and age-matched non-transgenic WT mice.

## Results

### Cognitive behavior

#### *Rotarod test*

To determine whether mutant tau affects coordination and motor skill acquisition, using rotarod, we assessed motor learning and coordination. We found significantly reduced latency to fall on an accelerating rotarod test was in 12-month-old tau mice ($P = 0.002$) relative non-transgenic WT mice (Fig. 1A), indicating that impairments in motor learning and coordination. As shown in Figure 1A, the latency to fall in all four trails was consistent in tau mice, suggesting that impairments in motor learning and coordination were progressive.

#### *Morris water maze test*

#### *Latency to find platform*

To determine hippocampal dependent learning and memory in tau and WT mice, we performed hidden-platform MWM test. As shown in Figure 1B, tau mice showed an increase in escape latency to find the hidden platform during training between trials 7 and 16 relative to WT mice. The average latency time to find platform was significantly increased in tau mice ($P = 0.0001$) compared with WT mice. These observations indicate that an impairment of learning and memory in tau mice.

#### *Swimming speed*

As shown in Figure 1C, tau mice displayed a declined motor ability in MWM test, indicated by a gradually decreased swimming speed relative to WT mice. Average swimming speed was significantly decreased in tau mice ($P = 0.0001$) compared with WT mice.

#### *Time spent in target quadrant*

As shown in Figure 1D, during the probe trail, tau mice spent reduced time in all 16 trials on target quadrant compared with WT mice. Average time spent in target quadrant was significantly decreased in tau mice ($P = 0.0001$) compared with WT mice.

These observations strongly suggest that mutant tau and/or phosho tau is responsible impairment in overall cognitive behavior.

### Immunoblotting analysis

To understand the toxic effects of mutant tau on mitochondrial dynamics, we performed immunoblotting analysis of mitochondrial fission proteins, Drp1 and Fis1 and mitochondrial fusion proteins Mfn1, Mfn2 and opa1 in hippocampal tissues from 12-month-old tau and age-matched WT mice.

As shown in Figure 2A and B, significantly increased levels of fission proteins Drp1 ($P = 0.003$) and Fis1 ($P = 0.01$) were found in hippocampal tissues from 12-month-old tau mice relative to age-matched WT mice. On the contrary, mitochondrial fusion proteins, Mfn1 ($P = 0.002$), Mfn2 ($P = 0.003$) and Opa1 ($P = 0.01$) were significantly decreased in hippocampal tissues from tau mice relative to WT mice. These observations indicate that accumulation of hippocampal phosphorylated tau caused impaired mitochondrial dynamics in tau mice.

To determine the toxic effects of mutant tau on dendritic protein, MAP2 and tau phosphorylation, we quantified total tau, phosphorylated tau 181 and 231 and MAP2 proteins from hippocampal tissues of 12-month-old tau and WT mice.

In tau mice relative to WT mice, significantly decreased level of MAP2 ($P = 0.03$). As shown in Figure 3A and B, significantly

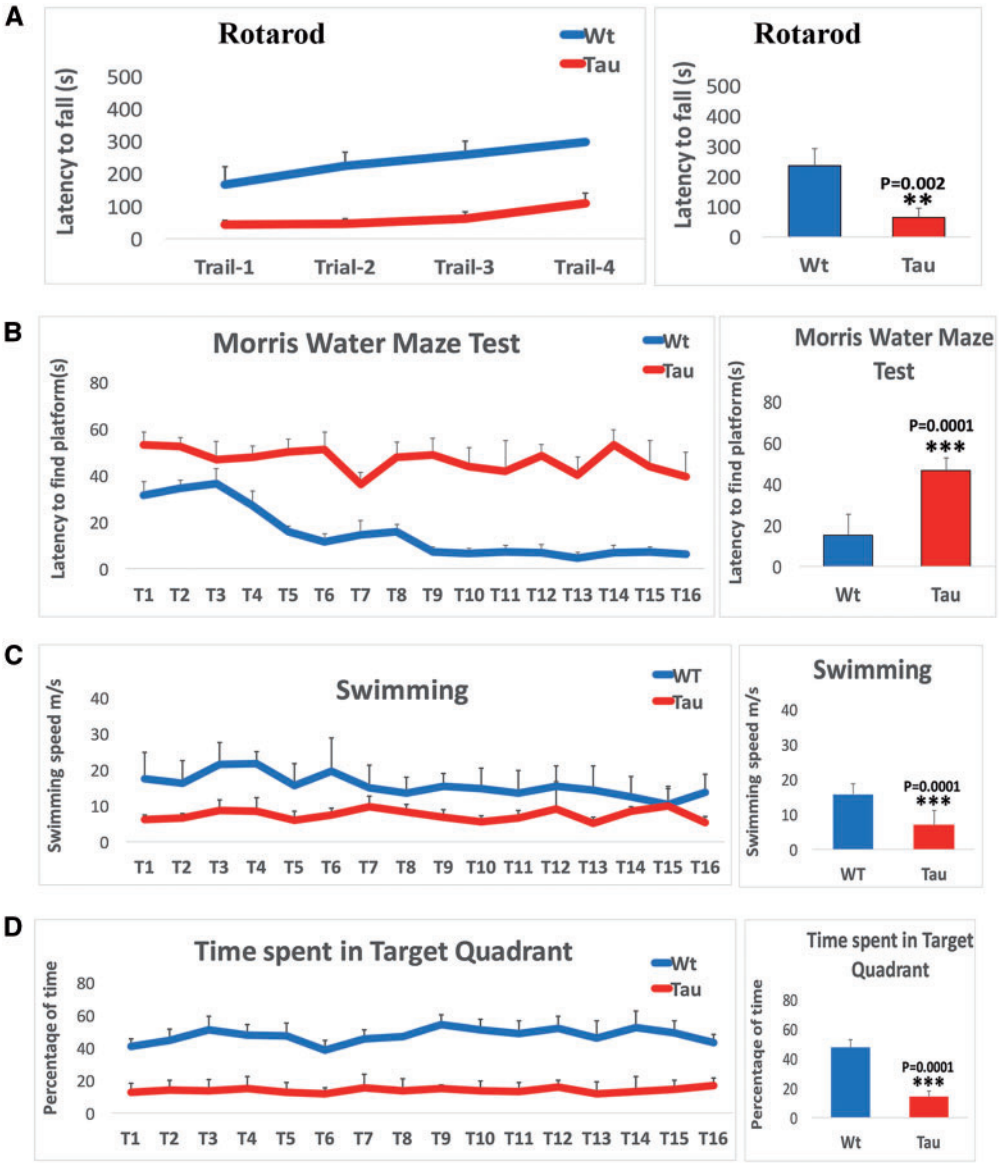


**Figure 1.** Cognitive behavior in 12-month-old tau and non-transgenic wild-type (WT) mice. (**A**) Rotarod test in 12-month-old tau mice ($n = 15$) and non-transgenic WT mice ($n = 15$). (**B**) Latency to find platform test in 12-month-old tau and non-transgenic WT mice. (**C**) Swimming speed in 12-month-old tau and non-transgenic WT mice. (**D**) Time spent target quadrant in 12-month-old tau and non-transgenic WT mice. *Rotarod*: significantly reduced latency to fall on an accelerating rotarod test was found in 12-month-old tau mice ($P$=0.001) relative non-transgenic WT mice (A) and the latency to fall in all four trails was consistent in tau mice, suggesting that impairments in motor learning and coordination was progressive. *Morris Water Maze test*: an increase in escape latency to find the hidden platform during training between trials 7 and 16 relative to WT mice and the average latency time to find platform was significantly increased in tau mice ($P$=0.0001) compared with WT mice (B). *Swimming speed*. Tau mice displayed a gradually decreased swimming speed relative to WT mice and an average swimming speed was significantly decreased in tau mice ($P$=0.0001) compared with WT mice (C). Tau mice spent reduced time in all 16 trials on target quadrant compared with WT mice and average time spent in target quadrant was significantly decreased in tau mice ($P$=0.0001) compared with WT mice (D).

increased levels of total tau ($P = 0.03$), phosphorylated tau 181 ($P = 0.04$) and phosphorylated tau 231 ($P = 0.003$) were found in 12-month-old tau mice relative to age-matched non-transgenic WT mice.

We also assessed ratio between total tau and phosphorylated tau for tau and WT mice. Tau mice showed increased ratio of phosphorylated tau181/total tau (0.7–1.0) and phosphorylated tau231 (0.7–1)/total tau compared with WT mice phosphorylated tau181/total tau (0.4–1), phosphorylated tau231 (0.4–1). These observations indicate that mutant tau affects dendritic protein and tau phosphorylation.

## Immunofluorescence analysis

Using immunofluorescence analysis, localizations and levels of MAP2 and total and phosphorylated tau proteins (phospho-tau 181 and phospho-tau 231) were assessed in hippocampal sections from 12-month-old tau and WT, mice.

As shown in Figure 4, significantly decreased levels of MAP2 ($P = 0.01$) were found in tau mice relative to WT mice, indicating that mutant tau reduces MAP2 in tau mice.

Significantly increased levels of total tau ($P = 0.004$), phospho-tau 181 ($P = 0.001$) and phospho-tau 231 ($P = 0.003$) in 12-month-old tau mice relative to age-matched WT mice

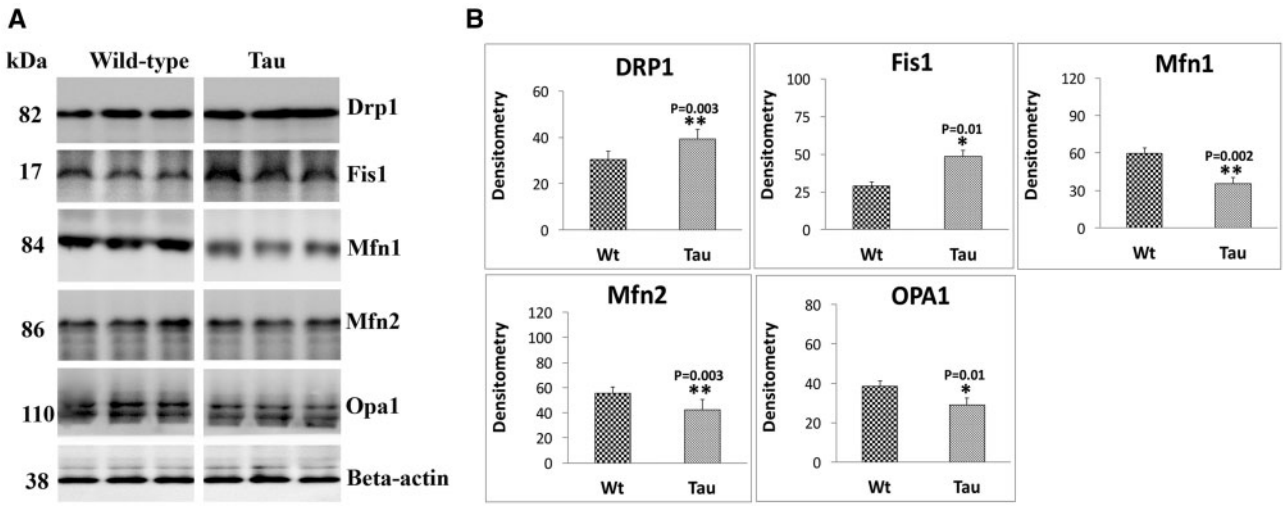


Figure 2. Immunoblotting analysis of mitochondrial dynamics proteins in 12-month-old tau and non-transgenic wild-type (WT) mice. (A) Representative immunoblotting analysis of 12-month-old tau and WT mice. (B) Quantitative densitometry analysis of mitochondrial dynamics proteins Drp1, Fis1 (fission) and Mfn1, Mfn2 and Opa1 (fusion). Protein levels of Drp1 ($P = 0.003$), Fis1 ($P = 0.01$) were significantly increased; and Mfn1 ($P = 0.002$), Mfn2 ($P = 0.003$) and Opa1 ($P = 0.01$) were significantly decreased in tau mice relative to WT mice.

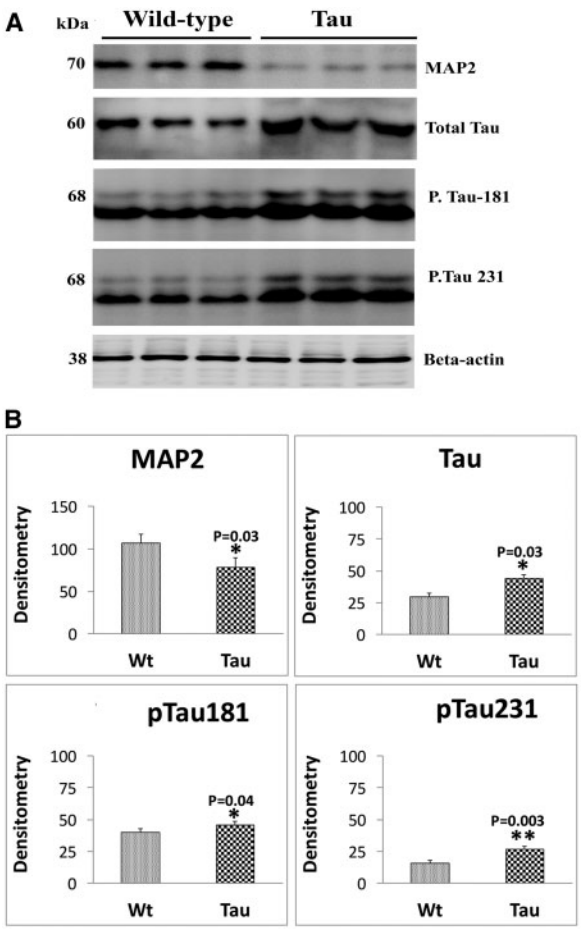


Figure 3. Immunoblotting analysis of dendritic protein MAP2 and tau proteins in 12-month-old tau and non-transgenic WT mice. (A) Representative immunoblotting analysis of 12-month-old tau and WT mice. (B) Quantitative densitometry analysis of mitochondrial dynamics proteins MAP2, total tau, phospho-tau 181 and phospho-tau 231. Dendritic protein MAP2 ($P = 0.02$) was significantly decreased; and total tau ($P = 0.03$), phospho-tau 181 ($P = 0.04$) and phosphorylated 231 ($P = 0.003$) were significantly increased in tau mice relative to WT mice.

(Fig. 5A and B), indicating that mutant tau enhances hyperphosphorylation of tau in tau mice.

## Dendritic spines

To determine the effects of mutant tau on dendritic spines, we quantified dendritic spines using Golgi-Cox staining in hippocampus of 12-month-old tau and age-matched WT mice.

As shown in Figure 6, we found significantly reduced dendritic spines in tau mice ($P = 0.0001$) relative to WT mice, indicating that hyperphosphorylated tau reduces dendritic spines in tau mice.

## Mitochondrial function

Mitochondrial function was assessed in hippocampus of 12-month-old tau mice and age-matched WT mice by measuring hydrogen peroxide, lipid peroxidation, cytochrome c oxidase activity and mitochondrial ATP.

### *$H_2O_2$ production*

As shown in Figure 7A, significantly increased levels of hydrogen peroxide ($H_2O_2$) were found in 12-month-old tau mice relative to WT mice ($P = 0.003$), indicating that mutant tau increases $H_2O_2$ levels in tau mice.

### *Lipid peroxidation*

Similar to hydrogen peroxide, levels of 4-hydroxy-2-nonenol, an indicator of lipid peroxidation, were significantly increased in tau mice ($P = 0.002$) relative to WT mice (Fig. 7B).

### *Cytochrome c oxidase activity*

Significantly decreased levels of cytochrome oxidase activity were found in 12-month-old tau mice ($P = 0.01$) relative to WT mice (Fig. 7C), indicating that mutant tau reduces cytochrome oxidase activity in tau mice.

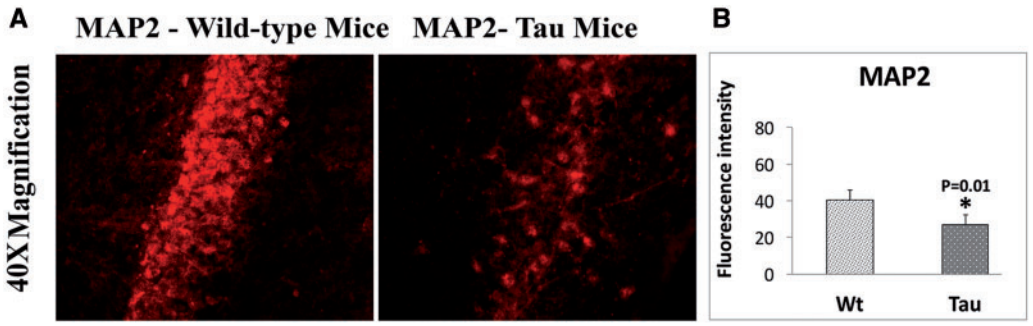


**Figure 4.** Immunofluorescence analysis of dendritic protein MAP2 protein in 12-month-old tau and non-transgenic WT mice. (**A**) Immunofluorescence analysis. (**B**) Quantitative immunofluorescence analysis. The MAP2 was significantly decreased in 12-month-old tau mice ($P = 0.01$) relative to WT mice.

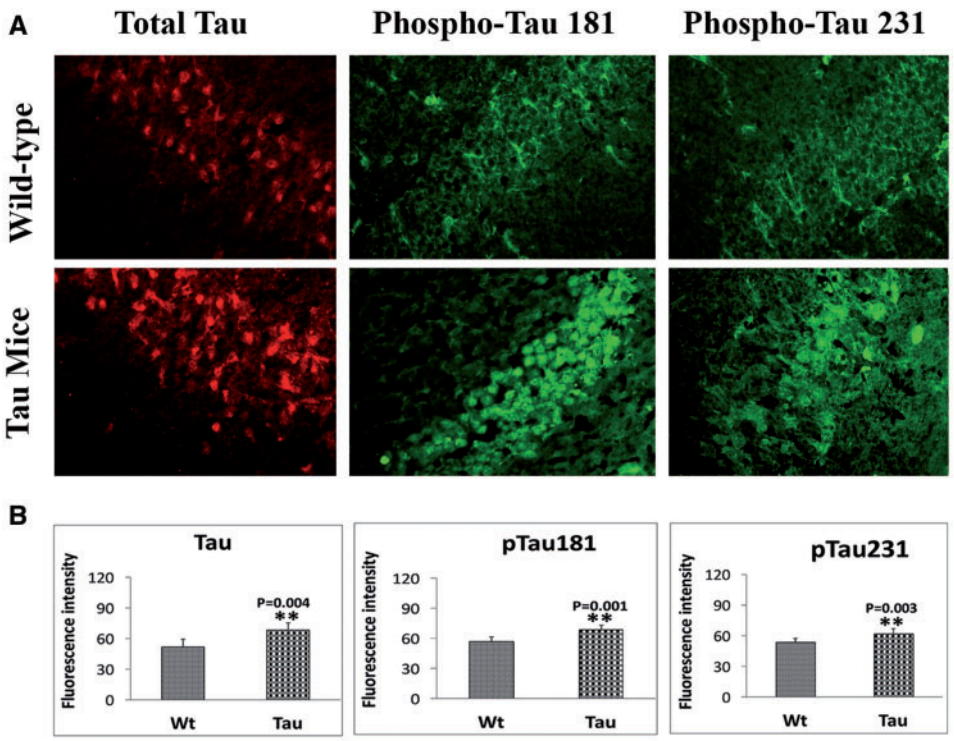


**Figure 5.** Immunofluorescence analysis of total and phosphorylated proteins in 12-month-old tau and non-transgenic wild-type (WT) mice. (**A**) Immunofluorescence analysis. (**B**) Quantitative immunofluorescence analysis. Significantly increased levels of total tau ($P = 0.004$), phospho-tau 181 ($P = 0.001$) and phospho-tau 231 ($P = 0.003$) in 12-month-old tau mice relative to WT mice.

*ATP production*

As shown in Figure 7D, significantly decreased levels of mitochondrial ATP were found tau mice relative to WT mice ($P = 0.001$), indicating that mutant tau affects mitochondrial ATP in tau mice.

## Transmission electron microscopy

To determine the effects of mutant tau on mitochondrial number and length, we used TEM on hippocampal and cortical tissues from 12-month-old tau mice and age-matched WT mice.

*Mitochondrial number in hippocampus*

As shown in Figure 8A, we found significantly increased number of mitochondria in hippocampi of 12-month-old tau mice ($P = 0.001$) relative to age-matched WT mice, suggesting that mutant tau fragments hippocampal mitochondria.

*Mitochondrial length in hippocampus*

We also measured mitochondrial length in order to understand whether mutant tau alters mitochondrial length. As shown in Figure 8A, we found mitochondrial length is significantly decreased in hippocampal tissues from tau mice ($P = 0.004$) relative to WT mice.

*Mitochondrial number in cerebral cortex*

As shown in Figure 8A, we found significantly increased number of mitochondria in cortical tissues of 12-month-old tau mice ($P = 0.002$) relative to age-matched WT mice, suggesting that mutant tau fragments cortical mitochondria.

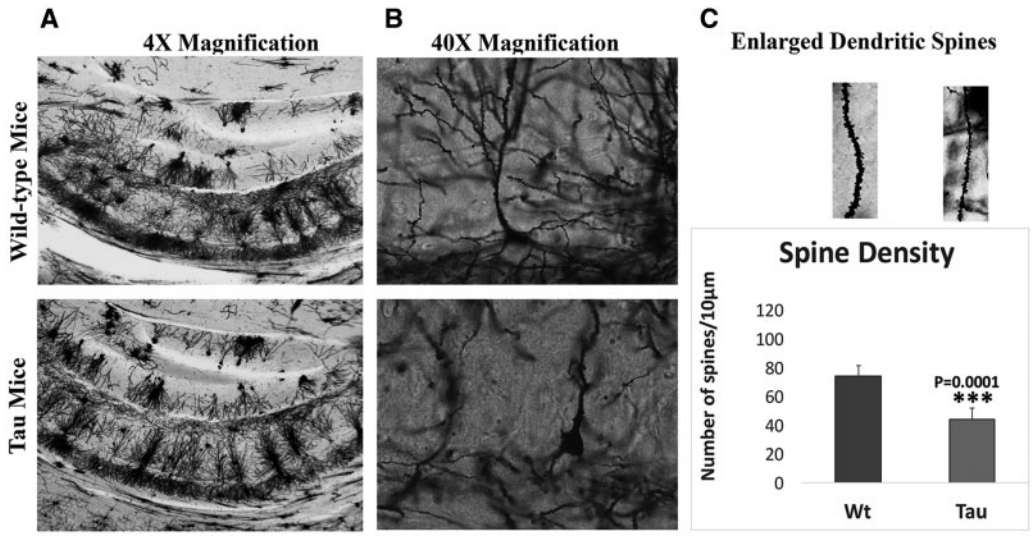


Figure 6. Hippocampal dendritic spine density in 12-month-old tau and non-transgenic WT mice. (A) Low magnification of Golgi-Cox staining. (B) Enlarged neuron with dendrites and (C) quantification of spine density in tau and WT mice. Significantly reduced dendritic spines were found in tau mice ($P = 0.0001$) relative to WT mice, indicating that hyperphosphorylated tau reduces dendritic spines in tau mice.

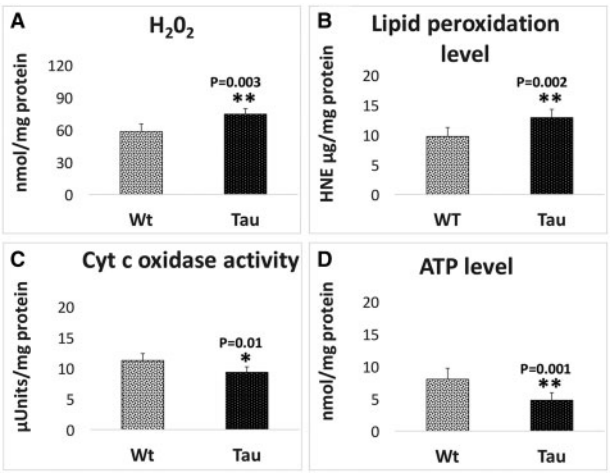


Figure 7. Mitochondrial functional parameters in 12-month-old tau and non-transgenic WT mice. Mitochondrial function was assessed by measuring: (A) $H_2O_2$ production, (B) lipid peroxidation, (C) cytochrome oxidase activity and (D) ATP levels. The levels of $H_2O_2$ ($P = 0.003$) and 4-hydroxy-2-nonenol ($P = 0.002$) were significantly increased and the levels of cytochrome oxidase ($P = 0.01$) and ATP ($P = 0.001$) significantly decreased found in tau mice relative to WT mice.

#### *Mitochondrial length in cerebral cortex*

We also measured mitochondrial length in order to understand whether mutant tau alters mitochondrial length. As shown in Figure 8B, we found mitochondrial length is significantly decreased in cortical tissues from tau mice ($P = 0.005$) relative to WT mice.

## Discussion

We investigated the toxic effects of phosphorylated tau, including cognitive behavior, levels of mitochondrial dynamics proteins, dendritic protein MAP2, total and phosphorylated tau proteins, dendritic spine density, mitochondrial number and length and mitochondrial function in 12-month-old tau mice. Using rotarod and MWM tests, immunoblotting and immunofluorescence, Golgi-Cox staining and transmission electron microscopy, we assessed cognitive behavior, measured protein levels of mitochondrial dynamics, MAP2, total and phosphorylated tau, quantified dendritic spines and studied mitochondrial number and number. Mitochondrial function was assessed by measuring the levels of $H_2O_2$, lipid peroxidation, cytochrome oxidase activity and mitochondrial ATP. MWM and rotarod tests revealed that hippocampal learning and memory and motor learning and coordination were impaired in tau mice. Increased levels of mitochondrial fission proteins and decreased levels of mitochondrial fusion proteins were found in 12-month-old tau mice relative to age-matched WT mice, indicating that the presence of abnormal mitochondrial dynamics in tau mice. Decreased levels of MAP2 and increased levels of total and phosphorylated tau proteins were found in 12-month-old tau mice relative to WT mice. Mitochondrial dysfunction was defective. Golgi-Cox staining analysis revealed that dendritic spines are significantly reduced. Transmission electron microscopy revealed significantly increased mitochondrial numbers and reduced mitochondrial length in tau mice. These findings suggest that a phosphorylated tau is responsible for cognitive decline, reduced dendritic protein, MAP2 and dendritic spine density and mitochondrial structural and functional changes.

Current study observations of increased mitochondrial fragmentation agree with findings from multiple lines of APP transgenic mice (22–24), strongly suggest that mitochondrial fragmentation is a typical feature of AD—meaning excessive fragmentation of mitochondria is observed in both APP and tau mice. Interestingly, the excessive mitochondrial fragmentation was reduced in several lines of APP mice treated with mitochondrial division inhibitor 1 (Mdvi1) (23,24). These observations strongly indicate that Mdivi1 is a promising therapeutic drug for AD.

### Hippocampal phosphorylated tau-induced cognitive behavior

Amyloid beta deposits and NFTs are the major pathological hallmarks of AD, but these features do not correlate with cognitive

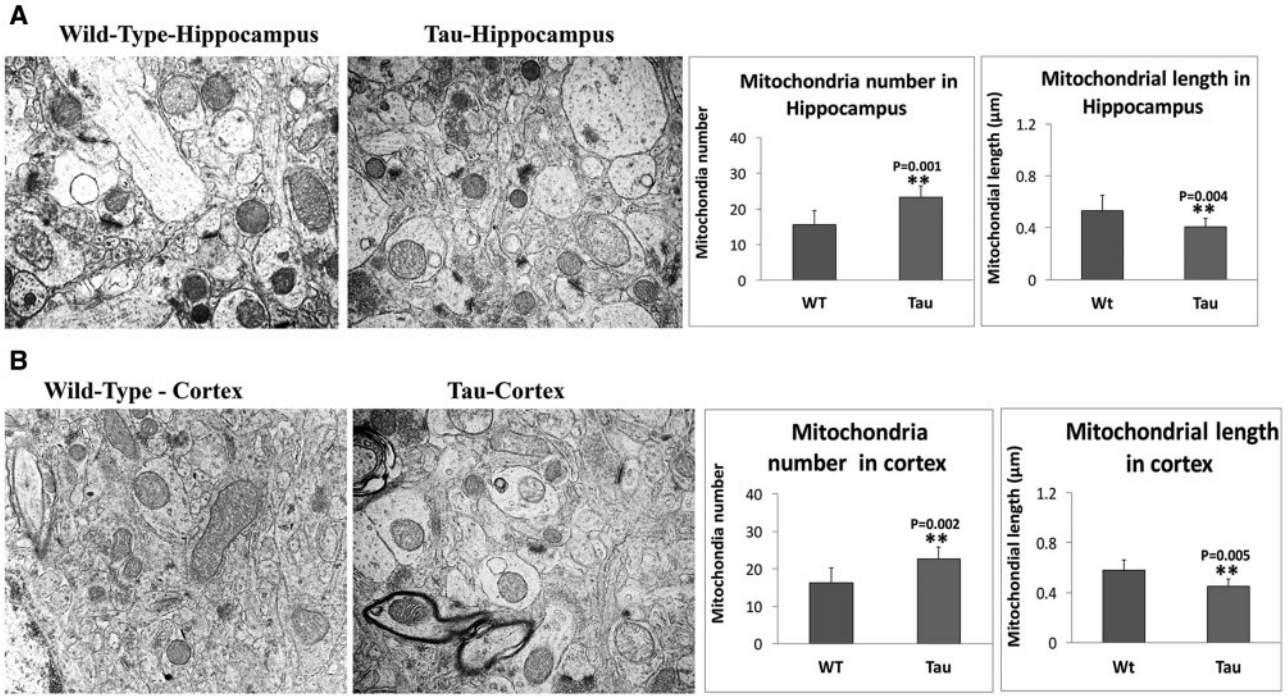


**Figure 8.** Mitochondrial number and length in 12-month-old tau and non-transgenic WT mice. (**A**) Mitochondrial number and length in hippocampus of tau mice and WT mice. (**B**) Mitochondrial number and length in cortex of tau and WT mice. Significantly increased number of mitochondria were found in the hippocampi of 12-month-old tau mice ($P = 0.001$) relative to age-matched WT mice, suggesting that mutant tau fragments hippocampal mitochondria. On the contrary, mitochondrial length is significantly decreased in the hippocampal tissues from tau mice ($P = 0.004$) relative to WT mice (A). Significantly increased number of mitochondria in cortical tissues of 12-month-old tau mice ($P = 0.002$) relative to age-matched WT mice. Mitochondrial length is significantly decreased in cortical tissues from tau mice ($P = 0.005$) relative to WT mice.

decline in patients with AD (5). However, loss of dendritic spines and synaptic damage are the best correlates of cognitive decline in AD patients and AD mice. Recent research also revealed that accumulation of phosphorylated tau in affected regions of the brain including hippocampus and cortex causes damage to synapses and responsible for cognitive decline in AD. Therefore, we focused on hippocampal tau accumulation, dendritic protein MAP2, dendritic spines, mitochondrial dynamics proteins and mitochondrial structural and functional changes—more importantly hippocampal tau-induced cognitive behavior using mice that express mutant tau with P301L mutation.

The spatial learning in the MWM is sensitive to hippocampal impairment (19–21) and that it is affected by phosphorylated tau accumulation (25–28). In the current study, we studied MWM primarily to understand the links between tau accumulation in hippocampus and spatial learning and memory in 12-month-old tau mice. We found that tau mice exhibit longer time to reach the platform, which is considered to be a specific neurocognitive performance measure. Further, animals in swimming test, displayed decreased swimming speed in all 16 trials relative to WT mice. Average swimming speed was significantly decreased in tau mice compared with WT mice. Further, time spent in target quadrant is also reduced in tau mice. Average time spent in target quadrant was significantly decreased in tau mice ($P = 0.0001$) compared with WT mice. Findings from these MWM test suggests that hippocampal accumulated tau is responsible for defects in spatial learning in tau mice.

On an accelerating rotarod test, tau mice displayed reduced latency to fall relative to non-transgenic WT mice, indicating that impairments in motor learning and coordination. The advantage of this test is that it creates a discretely measurable, continuous variable length of time that can be used to quantify the effects of accumulated mutant tau in hippocampus mice.

Overall, these behavioral impairments together with increased levels of accumulated tau in hippocampus and reduced hippocampal dendritic spines strongly suggest that hippocampal tau accumulations are responsible for defective learning and memory and motor coordination in tau mice.

## Hippocampal phosphorylated tau-induced dendritic proteins and spine density

It is well established that spine density is critical for synaptic function and cognitive behavior in AD patients and AD mice. In the current study, we found increased total and phosphorylated tau at hippocampal region of tau mice. As described earlier, we assessed dendritic spines and dendritic protein MAP2, in the hippocampi of tau mice. We found significantly reduced dendritic protein MAP2 (Fig. 3), and dendritic spines (Fig. 6) in tau mice relative to WT mice, indicating that hippocampal phosphorylated tau may be responsible for reduced dendritic spines and reduced dendritic protein MAP2, in tau mice.

## Hippocampal phosphorylated tau-induced impaired mitochondrial dynamics and mitochondrial structural and functional changes

It is well-established that structurally damaged mitochondria are present in AD neurons and in the primary neurons from AD mice, particularly at nerve terminals (29). We found increased fission and decreased fusion proteins in 12-month-old tau mice,

indicating that impaired mitochondrial dynamics is present in tau mice. These structurally damaged mitochondria are dysfunctional and may not produce ATP at synapses, leading to synaptic damage. To understand mitochondrial structural and functional changes, we assessed mitochondrial number and length in hippocampal and cortical regions of tau mice. We found significantly increased number of mitochondria in hippocampal and cortical tissues of 12-month-old tau mice relative to age-matched WT mice (Fig. 8) suggesting that phosphorylated tau accumulation fragments hippocampal (Fig. 8A) and cortical (Fig. 8B) mitochondria. As expected mitochondrial length was significantly decreased in hippocampal and cortical tissues from tau mice. Accumulation of phosphorylated tau is responsible for impaired mitochondrial dynamics (increased fission and decreased fusion) and mitochondrial structural abnormalities in tau mice. Our present study findings agree with a previous study of diabetic/obese rats by Choi *et al.* (30). They studied the effects of accumulation of phosphorylated tau in hippocampal mitochondria on cognitive behavior. They found cognitive behavioral impairments in diabetic/obese rats, suggesting that hippocampal accumulation of phosphorylated tau is responsible for cognitive deficits found in diabetic/obese rats (30).

In tau mice, mitochondrial function was found to be defective (Fig. 7). Our observations agree with others on hyperphosphorylated-induced defective mitochondrial function. Lipid peroxidation and hydrogen peroxide levels were significantly increased in hippocampal region of the brain in tau mice. On the contrary, cytochrome oxidase activity and mitochondrial ATP were reduced in tau mice. It is interesting to note that phosphorylated tau is significantly increased in hippocampal region in tau mice, further strengthening our notion that hyperphosphorylated tau is responsible for mitochondrial and synaptic toxicities (reduced dendritic protein MAP2 and spine density) in tau mice.

In summary, our study observations suggest that hippocampal accumulation of phosphorylated tau is responsible for (i) cognitive impairments, (ii) abnormal mitochondrial dynamics (increased fission and decreased fusion), (iii) loss of dendritic protein MAP2, (iv) dendritic spine density loss, (v) mitochondrial structural and functional changes, (vi) synaptic damage and (vii) neuronal dysfunction in tau mice. Our observations strongly suggest that reduced hippocampal hyperphosphorylated tau is an important therapeutic strategy for AD and other tauopathies.

## Materials and Methods

### Mutant tau mice

P301L mice were generated with human tau P301L mutation since this mutation is consistent with features of Tau found in persons with AD. These mice developed age-dependent hyperphosphorylated NFTs in the neocortex, the hippocampus and the cortex, where such NFTs have been found in persons with AD. Cognitive impairments were found in these homozygous mice at 4.5 months of age and at 6 months of age in the hemizygous mice. We purchased P301L mice from Taconic Farms (Rode Island, MA, USA) and used them for all of our study. We genotyped them for the human tau P301L mutation, using the DNA prepared from tail biopsy and PCR amplification, as described in Lewis *et al.* (31). Animals were euthanized before experimentation, according to procedures for euthanasia approved by the TTUHSC-IACUC.

We used 15, 12-month-old tau mice and 15 age-matched non-transgenic WT mice for behavioral studies and 10 tau mice and 10 WT mice for remaining studies, including immunoblotting, immunofluorescence, Golgi-Cox staining, mitochondrial function and transmission electron microscopy in our study.

### Behavioral tests

#### *Rotarod test*

The general motor function was assessed by using a single mouse rotarod (MedAssociates, Inc.). The animals were placed on the rotarod one after the other facing away from the experimenter and the apparatus set to gradually increased from 2 to 40 rpm over the course of 300 s. When the animal falls, an IR beam is broken, stopping the motor and the timer. The time for each trial was recorded, with a maximum of 300 s. Mice were then removed and allowed to rest for 30 min until returning to the remaining two sessions of the test, yielding a total of three trials a day for three consecutive days. Evaluation was made by monitoring latency to fall and maximal rotation rate before the mouse fell down. A soft pad was placed under the equipment as a precautionary measure against physical damages from falls.

### Morris water maze

The MWM apparatus (Coulborn Instruments, Allentown, PA, USA) in our laboratory were based on the design of Morris (32). This MWM was used to assess for studying different aspects of spatial memory (e.g. working memory); and non-spatial discrimination learning in tau mice with respect to the WT mice. The MWM apparatus consists of a 183-cm diameter pool filled with water to a depth of 48 cm and water temperature was maintained at 20 °C. The platform (18 cm diameter) was placed in the pool ∼2 cm below the surface of the water in one of the four quadrants. On the four sides of MWM apparatus different shapes of visual cues were placed inside the wall of the pool in a diagonal pattern. The water in the pool was made opaque to obscure the platform location using non-toxic white tempura paint (Utrecht Art Supplies, Cranbury, NJ, USA). We used tracking software (Actimetrics, Wilmette, IL, USA) to monitor and record each trial. In our MWM paradigm consisted of four 60-s trials per day for four consecutive days followed by reference memory probe trials after training. At end of each trial mouse was dried with dry cloth and retuned back to the home cage which was kept on heating pad. The interval for each trial mouse was ∼10 min. For each trial, pre-determined starting position was different and allowed to swim while being tracked by the software. The trial ended when the animal found the platform or when 60 s had elapsed. If the mouse did not reach the platform, it was placed onto the platform and left there for 10 s. Reference memory probe trials consisted of a single 60-s free swim from a single-start point. The platform was removed for the probe trial but its previous location was recorded with the monitoring software. A 60-s probe trial was performed on the fourth day to determine memory retention. For this single trial, the submerged platform was removed and each mouse was placed into the quadrant opposite to the quadrant that formerly contained the platform in acquisition testing. The number of annulus crossings, the percentage of time spent in each quadrant and average swim speed was determined from the retrieved videotapes. All behavioral studies were conducted in a double blinded manner.

### Immunoblotting analysis

To determine whether mutant tau alters the protein levels of mitochondrial fission (Drp1 and Fis1) and fusion (Mfn1, Mfn2 and Opa1) dendritic protein, MAP2 and increases phosphorylated we performed immunoblotting analyses of protein lysates from 12-month-old tau, and WT mice as described in Manczak *et al.* (33). We also assessed total, phosphorylated tau levels in tau mice relative to WT mice. Twenty micrograms of protein lysates from hippocampal tissues of all lines mice were resolved on a 4–12% Nu-PAGE gel (Invitrogen). The resolved proteins were transferred to nylon membranes (Novax, Inc., San Diego, CA, USA) and were then incubated for 1 hour at room temperature with a blocking buffer (5% dry milk dissolved in a TBST buffer). The nylon membranes were incubated overnight with the primary antibodies (Drp1–1:500 rabbit-polyclonal, Novus Biologicals, Littleton, CO, USA; 1:500, rabbit polyclonal of Fis1, Protein Tech Group, Inc., Chicago, IL, USA; Mfn1–1:400 rabbit polyclonal Abcam, Cambridge, MA, USA; Mfn2–1:400 rabbit polyclonal, Abcam; Opa1–1:500 BD Biosciences, San Jose, CA, USA; MAP2–1:500 dilutions, Santa Cruz Biotechnology, Dallas, USA; Total Tau (1:200), Phospho Tau 181 (1:200), Phospho Tau 231 (1:200), Thermoscientific. The membranes were washed with a TBST buffer 3 times at 10-min intervals and were then incubated for 2 h with appropriate secondary antibodies (1:5000 dilutions of Anti mouse IgG HRP; Anti-rabbit IgG HRP, GE Health Care life Sciences, Pittsburgh, USA), followed by three additional washes at 10-min intervals. Proteins were detected with chemilumniscence reagents (Pierce Biotechnology, Rockford, IL, USA), and the bands from immunoblots were quantified on a Kodak Scanner (ID Image Analysis Software, Kodak Digital Science, Kennesaw, GA, USA). Briefly, image analysis was used to analyze gel images captured with a Kodak Digital Science CD camera. The lanes were marked to define the positions and specific regions of the bands. An ID fine-band command was used to locate and to scan the bands in each lane and to record the readings.

### Immunofluorescence analysis and quantification of MAP2, total tau and phosphorylated tau in 12-month-old tau mice

Immunofluorescence analysis was performed using midbrain sections from tau, and WT mice as described in Manczak *et al.* (33). The midbrain sections tau and WT mice were washed with warm PBS, fixed in freshly prepared 4% paraformaldehyde in PBS for 10 min, and then washed with PBS and permeabilized with 0.1% Triton X-100 in PBS. They were blocked with a 1% blocking solution (Invitrogen) for 1 h at room temperature. All sections were incubated overnight with primary antibodies (1:300 dilutions of MAP2, Santa Cruz Biotechnology; total tau, Thermoscientific, phospho-tau 181, phospho-tau 231, Novus Biologicals). After incubation, the sections were washed 3 times with PBS, for 10 min each. The sections were incubated with a secondary antibody conjugated with Flours 488 (Ref# A21206, Molecular Probes, Eugene, OR, USA) and 594 (Ref# A21203, Molecular Probes) for 1 h at room temperature. The sections were washed three times with PBS and mounted on slides. Photographs were taken with a multiphoton laser scanning microscope system (ZeissMeta LSM510). To quantify the immunoreactivity of mitochondrial and synaptic antibodies for each treatment, 10–15 photographs were taken at ×40 magnifications, and statistical significance was assessed, using one-way ANOVA for proteins.

### Golgi-Cox staining and dendritic spine count

Golgi-Cox impregnation has been one of the most effective techniques for studying both the normal and abnormal morphology of neurons. The morphology of neuronal dendrites and dendritic spines have been discovered in the brains of mice by using Golgi-Cox staining and it was performed by using the FD Rapid GolgiStain Kit (FD Neuro Technologies, Columbia, MD, USA). Briefly, animals were anaesthetized before killing and brains from the mice skull were removed carefully as quickly as possible. The intact mice brain tissues were rinsed with Milli Q water to remove blood from the surface. The mice brain tissues were impregnated in the equal volumes of Solutions A and B, the impregnation solution was replaced the following day and stored at room temperature for 2 weeks in the dark. The brains were transferred to Solution C after 2 weeks. The Solution C was replaced the following day and the brains were stored at 4 °C for 72 h in the dark. The Brain sections (100 μm thickness) were generated using a cryotome with the chamber temperature set at −22 °C. Each section was mounted on gelatin-coated microscope slides using Solution C. The excess solution on slide was removed with a Pasteur pipette and then absorbed with stacks of filter paper, and the sections were allowed to dry naturally at room temperature (3 days). The dried brain sections were processed as per the manufacturer's instructions. Briefly, dendrites within the CA1 sub region of the hippocampus were imaged using a 4×, 20× and 40×, 64× objectives using EVOS microscope-AMG (thermofisher.com) and Olympus1X71, respectively. Dendritic spines were detected along CA1 secondary dendrites starting from their point of origin on the primary dendrite and the counting was performed by an experimenter blinded to the group of each sample (34).

### Transmission electron microscopy

To determine the effects of phosphorylated tau on the mitochondrial number and size, we performed transmission electron microscopy in hippocampal and cortical sections of 12-month-old tau mice relative to age-matched WT mice. Animals were perfused using standard perfusion method—after successful perfusion, skin was removed on top of head and take the brain out, and post-fixed the brain for 2–3 h and/or definitely, and cut the hippocampal and cortical sections for transmission electron microscopy. 1× 1 mm thickness fixed sections from hippocampi and cortices were used for further analysis. Cut sections were stained for 5 min in lead citrate. They were rinsed and post-stained for 30 min in uranyl acetate and then were rinsed again and dried. Electron microscopy was performed at 60 kV on a Philips Morgagni TEM equipped with a CCD, and images were collected at magnifications of ×1000–37 000. The numbers of mitochondria were counted and statistical significance was determined, using one-way ANOVA.

### Mitochondrial functional assays

#### *$H_2O_2$ production*

Using an Amplex® Red H2O2 Assay Kit (Molecular Probes), the production of $H_2O_2$ was measured using hippocampal tissues from 12-month-old tau mice and WT mice as described in Kandimalla *et al.* (35). Briefly, $H_2O_2$ production was measured in the mitochondria hippocampal tissues from all four lines of mice. A BCA Protein Assay Kit (Pierce Biotechnology) was used to estimate protein concentration. The reaction mixture contained mitochondrial proteins (μg/μl), Amplex Red reagents

(50 μM), horseradish peroxidase (0.1 U/ml), and a reaction buffer (1×). The mixture was incubated at room temperature for 30 min, followed by spectrophotometer readings of fluorescence (570 nm). Finally, $H_2O_2$ production was determined, using a standard curve equation expressed in nmol/μg mitochondrial protein. Hydrogen peroxide levels were compared between tau and mice.

#### *Lipid peroxidation assay*

Lipid peroxidates are unstable indicators of oxidative stress in the brain. The final product of lipid peroxidation is 4-hydroxy-2-nonenol (HNE), which was measured from hippocampal tissues from tau and WT mice. We used HNE-His ELISA Kit (Cell BioLabs, Inc., San Diego, CA, USA) as described in Kandimalla *et al.* (35). Briefly, freshly prepared protein as added to a 96-well protein binding plate and incubated overnight at 4 °C. It was then washed three times with a buffer. After the last wash, the anti-HNE-His antibody was added to the protein in the wells, which was then incubated for 2 h at room temperature and was washed again three times. Next, the samples were incubated with a secondary antibody conjugated with peroxidase for 2 h at room temperature, followed by incubation with an enzyme substrate. Optical density was measured (at 450 nm) to quantify the level of HNE. Lipid peroxidation levels were compared between tau mice and WT mice.

#### *Cytochrome oxidase activity*

Cytochrome oxidase activity was measured in hippocampal tissues from all lines of mice. Enzyme activity was assayed spectrophotometrically using a Sigma Kit (Sigma–Aldrich) following the manufacturer's instructions (32). Briefly, 2 μg protein lysate was added to 1.1 ml of a reaction solution containing 50 μl 0.22 mM ferricytochrome *c* fully reduced by 0.1 M DTT, Tris–HCl (pH 7.0) and 120 mM potassium chloride. The decrease in absorbance at 550 mM was recorded for 1-min reactions at 10-s intervals. Cytochrome oxidase activity was measured according to the following formula: mU/mg total mitochondrial protein = [A/min sample − (A/min blank) × 1.1 mg protein × 21.84]. The protein concentrations were determined following the BCA method. Cytochrome *c* oxidase activity levels were compared between tau mice and WT mice.

#### *ATP levels*

ATP levels were measured in mitochondria isolated from hippocampal tissues of tau and WT mice and using ATP determination kit (Molecular Probes) (36). The bioluminescence assay is based on the reaction of ATP with recombinant firefly luciferase and its substract luciferin. Luciferase catalyzes the formation of light from ATP and luciferin. It is the emitted light that is linearly related to the ATP concentration, which is measured with a luminometer. ATP levels were measured from mitochondrial pellets using a standard curve method. ATP levels were compared between tau mice and WT mice.

## Acknowledgements

We sincerely thank all the staff at the animal facility for taking care of all lines of mice that are used in the study.

*Conflict of Interest statement*. None declared.

## Funding

Work presented in this article is supported by NIH grants AG042178, AG047812 and NS105473 and the Garrison Family Foundation and Alzheimer's Association SAGA grant (to P.H.R.).

## References

1. Mattson, M.P. (2004) Pathways towards and away from Alzheimer's disease. *Nature*, **430**, 631–639.
2. Bernstein, S.L., Dupuis, N.F., Lazo, N.D., Wyttenbach, T., Condron, M.M., Bitan, G., Teplow, D.B., Shea, J.E., Ruotolo, B.T. and Robinson, C.V. (2009) Amyloid-beta protein oligomerization and the importance of tetramers and dodecamers in the aetiology of Alzheimer's disease. *Nat. Chem.*, **1**, 326–331.
3. LaFerla, F.M., Green, K.N. and Oddo, S. (2007) Intracellular amyloid-beta in Alzheimer's disease. *Nat. Rev. Neurosci.*, **8**, 499–509.
4. Reddy, P.H. and Beal, M.F. (2008) Amyloid beta, mitochondrial dysfunction and synaptic damage: implications for cognitive decline in aging and Alzheimer's disease. *Trends Mol. Med.*, **14**, 45–53.
5. Reddy, P.H., Tripathi, R., Troung, Q., Tirumala, K., Reddy, T.P., Anekonda, V., Shirendeb, U.P., Calkins, M.J., Reddy, A.P., Mao, P. *et al.* (2012) Abnormal mitochondrial dynamics and synaptic degeneration as early events in Alzheimer's disease: implications to mitochondria-targeted antioxidant therapeutics. *Biochim. Biophys. Acta*, **1822**, 639–649.
6. Alzheimer's Association (2015) – Facts and Figures, 1–81.
7. Reddy, P.H. (2011) Abnormal tau, mitochondrial dysfunction, impaired axonal transport of mitochondria, and synaptic deprivation in Alzheimer's disease. *Brain Res.*, **1415**, 136–148.
8. Serrano-Pozo, A., Frosch, M.P., Masliah, E. and Hyman, B.T. (2011) Neuropathological alterations in Alzheimer disease. *Cold Spring Harbor Perspect. Med.*, **1**, a006189.
9. Selkoe, D.J. (2001) Alzheimer's disease: genes, proteins, and therapy. *Physiol. Rev.*, **81**, 741–766.
10. Reddy, P.H., Manczak, M., Mao, P., Calkins, M.J., Reddy, A.P. and Shirendeb, U. (2010) Amyloid-beta and mitochondria in aging and Alzheimer's disease: implications for synaptic damage and cognitive decline. *J. Alzheimers Dis.*, **20**, S499–S512.
11. Swerdlow, R.H., Burns, J.M., Khan, S.M., Zhu, X., Beal, M.F., Wang, X., Perry, G. and Smith, M.A. (2010) The Alzheimer's disease mitochondrial cascade hypothesis. *J. Alzheimers Dis.*, **20**, S265–S279.
12. Zhu, X., Perry, G., Smith, M.A. and Wang, X. (2013) Abnormal mitochondrial dynamics in the pathogenesis of Alzheimer's disease. *J. Alzheimers Dis.*, **33**, S253–S262.
13. Avila, J., Lucas, J.J., Perez, M. and Hernandez, F. (2004) Role of tau protein in both physiological and pathological conditions. *Physiol. Rev.*, **84**, 361–384.
14. Iqbal, K., Liu, F., Gong, C.X. and Grundke-Iqbal, I. (2010) Tau in Alzheimer disease and related tauopathies. *Curr. Alzheimer Res.*, **7**, 656–664.
15. Lee, V.M., Goedert, M. and Trojanowski, J.Q. (2001) Neurodegenerative tauopathies. *Annu. Rev. Neurosci.*, **24**, 1121–1159.
16. Brandt, R., Hundelt, M. and Shahani, N. (2005) Tau alteration and neuronal degeneration in tauopathies: mechanisms and models. *Biochim. Biophys. Acta*, **1739**, 331–354.
17. Mietelska-Porowska, A., Wasik, U., Goras, M., Filipek, A. and Niewiadomska, G. (2014) Tau protein modifications and

interactions: their role in function and dysfunction. *Int. J. Mol. Sci.*, **15**, 4671–4713.
18. Ittner, L.M. and Gotz, J. (2011) Amyloid-beta and tau–a toxic pas de deux in Alzheimer's disease. *Nat. Rev. Neurosci.*, **12**, 65–72.
19. Astur, R.S., Taylor, L.B., Mamelak, A.N., Philpott, L. and Sutherland, R.J. (2002) Humans with hippocampus damage display severe spatial memory impairments in a virtual Morris water task. *Behav. Brain Res.*, **132**, 77–84.
20. de Hoz, L., Moser, E.I. and Morris, R.G. (2005) Spatial learning with unilateral and bilateral hippocampal networks. *Eur. J. Neurosci.*, **22**, 745–754.
21. Goddyn, H., Leo, S., Meert, T. and Dhooge, R. (2006) Differences in behavioural test battery performance between mice with hippocampal and cerebellar lesions. *Behav. Brain Res.*, **173**, 138–147.
22. Wang, W., Yin, J., Ma, X., Zhao, F., Siedlak, S.L., Wang, Z., Fujioka, H., Xu, Y., Perry, G. and Zhu, X. (2017) Inhibition of mitochondrial fragmentation protects against Alzheimer's disease in rodent model. *Hum. Mol. Genet.*, **26**, 4118–4131.
23. Calkins, M.J., Manczak, M., Mao, P., Shirendeb, U. and Reddy, P.H. (2011) Impaired mitochondrial biogenesis, defective axonal transport of mitochondria, abnormal mitochondrial dynamics and synaptic degeneration in a mouse model of Alzheimer's disease. *Hum. Mol. Genet.*, **20**, 4515–4529.
24. Baek, S.H., Park, S.J., Jeong, J.I., Kim, S.H., Han, J., Kyung, J.W., Baik, S.H., Choi, Y., Choi, B.Y. and Park, J.S. (2017) Inhibition of Drp1 ameliorates synaptic depression, Aβ deposition, and cognitive impairment in an Alzheimer's disease model. *J. Neurosci.*, **37**, 5099–5110.
25. Arendash, G.W., Lewis, J., Leighty, R.E., McGowan, E., Cracchiolo, J.R., Hutton, M. and Garcia, M.F. (2004) Multi-metric behavioral comparison of APPsw and P301L models for Alzheimer's disease: linkage of poorer cognitive performance to tau pathology in forebrain. *Brain Res.*, **1012**, 29–41.
26. Ramsden, M., Kotilinek, L., Forster, C., Paulson, J., McGowan, E., SantaCruz, K., Guimaraes, A., Yue, M., Lewis, J. and Carlson, G. (2005) Age-dependent neurofibrillary tangle formation, neuron loss, and memory impairment in a mouse model of human tauopathy (P301L). *J. Neurosci.*, **25**, 10637–10647.
27. Schindowski, K., Bretteville, A., Leroy, K., Begard, S., Brion, J.P., Hamdane, M. and Buee, L. (2006) Alzheimer's disease-like tau neuropathology leads to memory deficits and loss of functional synapses in a novel mutated tau transgenic mouse without any motor deficits. *Am. J. Pathol.*, **169**, 599–616.
28. Rosenmann, H., Grigoriadis, N., Eldar-Levy, H., Avital, A., Rozenstein, L., Touloumi, O., Behar, L., Ben-Hur, T., Avraham, Y., Berry, E. *et al.* (2008) A novel transgenic mouse expressing double mutant tau driven by its natural promoter exhibits tauopathy characteristics. *Exp. Neurol.*, **212**, 71–84.
29. Wang, X., Wang, W., Li, L., Perry, G., Lee, H.G. and Zhu, X. (2014) Oxidative stress and mitochondrial dysfunction in Alzheimer's disease. *Biochim. Biophys. Acta*, **1842**, 1240–1247.
30. Choi, J., Chandrasekaran, K., Demarest, T.G., Kristian, T., Xu, S., Vijaykumar, K., Dsouza, K.G., Qi, N.R., Yarowsky, P.J., Gallipoli, R. *et al.* (2014) Brain diabetic neurodegeneration segregates with low intrinsic aerobic capacity. *Ann. Clin. Transl. Neurol.*, **1**, 589–604.
31. Lewis, J., McGowan, E., Rockwood, J., Melrose, H., Nacharaju, P., Van Slegtenhorst, M., Gwinn-Hardy, K., Paul Murphy, M., Baker, M., Yu, X. *et al.* (2000) Neurofibrillary tangles, amyotrophy and progressive motor disturbance in mice expressing mutant (P301L) tau protein. *Nat. Genet.*, **25**, 402–405.
32. Morris, R. (1984) Developments of a water-maze procedure for studying spatial learning in the rat. *J. Neurosci. Methods*, **11**, 47–60.
33. Manczak, M., Kandimalla, R., Fry, D., Sesaki, H. and Reddy, P.H. (2016) Protective effects of reduced dynamin-related protein 1 against amyloid beta-induced mitochondrial dysfunction and synaptic damage in Alzheimer's disease. *Hum. Mol. Genet.*, **25**, 5148–5166.
34. Gibb, R. and Kolb, B. (1998) A method for vibratome sectioning of Golgi-Cox stained whole rat brain. *J. Neurosci. Methods*, **79**, 1–4.
35. Kandimalla, R., Manczak, M., Fry, D., Suneetha, Y., Sesaki, H. and Reddy, P.H. (2016) Reduced dynamin-related protein 1 protects against phosphorylated Tau-induced mitochondrial dysfunction and synaptic damage in Alzheimer's disease. *Hum. Mol. Genet.*, **25**, 4881–4897.
36. Reddy, P.H., Manczak, M., Yin, X., Grady, M.C., Mitchell, A., Kandimalla, R. and Kuruva, C.S. (2016) Protective effects of a natural product, curcumin, against amyloid beta induced mitochondrial and synaptic toxicities in Alzheimer's disease. *J. Invest. Med.*, **64**, 1220–1234.